Scoping Environment for Robust 60 GHz Link Deployment

Sanjib Sur and Xinyu Zhang

University of Wisconsin-Madison

Email: sur2@wisc.edu, xyzhang@ece.wisc.edu

Abstract— Blockage by human body is a severe challenge to enabling robust 60 GHz directional links. Beam-steering may overcome this problem by electronically steering the signals, thus creating detour paths. However, effectiveness of beam-steering depends on the link's deployment location and the reflection characteristics of surrounding environment. An arbitrarily deployed link may suffer from complete black-out during human blockage. In this paper, we propose a new technique called *BeamScope*, that predicts the best possible deployment location in an indoor environment, without any explicit war-driving. *BeamScope* first characterizes the environment using sparse measurement from randomly deployed reference locations. It then predicts the link quality in unobserved locations to suggest a possible redeployment. More specifically, *BeamScope* characterizes the environment through a novel model that deems ambient reflectors as diffusive mirrors. It can extrapolate the reflectivity and geometrical parameters of the mirrors. Then, it predicts link quality by tracing the signal rays along their line-of-sight and reflecting paths. We have conducted preliminary evaluation of *BeamScope* on a 60 GHz software-radio testbed and a raytracing simulator. The results show promising accuracy in identifying the best possible locations for 60 GHz link to achieve robust connectivity.

I. INTRODUCTION

Millimeter-wave (mmWave) communication is the emerging frontier for next-generation wireless applications. With multi-Gbps data rate, it promises to trigger a new wave of data-hungry applications such as uncompressed video streaming, cordless computing, wireless projector, instant file synchronization, wireless fiber-to-home access, *etc*. The IEEE standards 802.11ad [1] and 802.15.3c [2], have ratified MAC/PHY protocols for communication via 60 GHz mmWave frequency, and have already been adopted in commercial devices [3]. Fig. 1 shows some of the potential indoor usage scenarios of 60 GHz networks.

Due to smaller wavelengths compared with the prevalent microwave band, 60 GHz links are inherently vulnerable to propagation loss. The standard protocols rely on narrow directional beams formed by phased-array antennas to overcome the strong signal attenuation. But, narrow directional beams are highly susceptible to human blockages that can occur in indoor deployments with heavy human activity [4]. A phased-array antenna can electronically steer its beam direction, bouncing the signals off opportunistic reflectors, thus detouring any Line-Of-Sight (LOS) obstacle. However, effectiveness of beam-steering depends highly on the environment, *e.g.*, availability of any secondary reflective paths [5].

At the core, any beam-steering algorithm is a *reactive* mechanism, which struggles to sustain the link when blockage occurs, but does not afford any *preventive* mechanism to reduce the likelihood of link outage during blockage. While deploying a 60 GHz link, current protocols are unable to
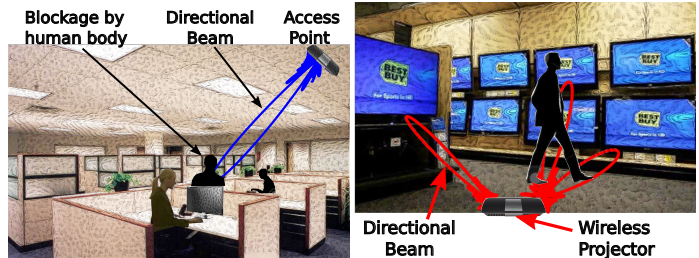

Fig. 1. Concept applications of 60 GHz. (a) Enterprise network. (b) Wireless Gbps projector.

determine whether the beam-steering can be effective in this setup. A "backup" beam approach, *i.e.*, availability of secondary beam before blockage may be used as an indicator of whether the link can be sustained. However, multiple beams can be often blocked simultaneously, even if their physical directions are different [6]. This phenomenon originates from the interplay between the *sparsity of 60 GHz channel* and the *phased-array beamforming*. Ideally, any preventive mechanism should be able to evaluate if a 60 GHz link is *robust* during deployment (*i.e.*, whether it can survive blockage using beam steering), and if not, suggest and guide the user for a possible re-deployment.

An obvious way to find out the best possible *spot* to deploy a 60 GHz link would be, to war-drive the entire deployment area covering every nook and cranny. But two problems render the war-driving ineffective: (1) *Overhead*. War-driving is a tedious and cumbersome process requiring labor effort. Even though an automated robot can be used to scour the place, physical *search space* involving possible combinations of transmitter/receiver locations can be quite large even for a small $10m \times 10m$ indoor room. (2) *Blockage incidences*. Exhaustive war-driving may specify best possible *spot* in a human-free indoor environment, but it does not consider possible blockage incidences and their patterns. One way to specify best possible *spot* is the one where maximum number of strong "backup" beam (in addition to the LOS beam) is available. But, owing to the spatial correlation between the phased-array beams [6] that involves beams sharing "invisible" reflective paths, backup beam approach rarely helps in blockage prevention and thus the notion of best *spot* becomes illusive during blockage.

In this paper, we propose *BeamScope*, a 60 GHz sensing mechanism that can find the best *spot* to place a 60 GHz link in an indoor environment, without any need for explicit war-driving. *BeamScope* is applicable to quasi-stationary 60 GHz links, which can be occasionally displaced, but frequently blocked by human waling by. *BeamScope* allows a pair of arbitrarily deployed 60 GHz transmitter and receiver to scope

the environment and predict the performance of unobserved *spots*. So, it can guide the user to place the nodes in the best available spots.

BeamScope builds on two key properties of 60 GHz links: *sparsity* of the channel response across spatial angles, and *spatial correlation* between links. *BeamScope* leverages the sparsity to fully characterize the environment from a single receiver viewpoint using only a few discrete paths, which we call *environment path skeleton*. More specifically, BeamScope constructs the environment path skeleton through a novel model that deems ambient reflectors as diffusive mirrors. It can extrapolate the reflectivity and geometrical parameters of the mirrors, which are shared among links and account for their correlation. Given the environment path skeleton, *BeamScope* predicts quality of unobserved link locations through a parametric composition of its LOS and reflecting paths. A strong environment change (*e.g.*, displacement of metallic furniture) may change the best spot. But *BeamScope* can recalibrate its modeling parameters according to the environment and guide the user for a possible re-deployment (if permitted).

We evaluate *BeamScope* using a combination of channel traces and simulation. The channel traces are collected on a 60 GHz software radio platform [5] that provides fine-grained spatio-temporal characteristics of 60 GHz links. We use a programmable motion control system and highly directional antennas (3°) to capture real link characteristics. The preliminary experimental results show that *BeamScope* can predict the spatial sparse channel and correspondingly performance of best beam in an unobserved spot utilizing measurement result from a reference spot. When using 32 phased-array beams, the prediction accuracy of identifying the best beam is 70% and its RSS is within 2 dB for 90 percentile confidence. Furthermore, we expect the prediction error to decrease further leveraging guided measurement of more reference sampling points and utilizing a more complete prototype, planned for future work.

The key contribution of *BeamScope* breaks down into the following two aspects.

(1) A measurement study to understand the impact of deployment locations on the robustness of a 60 GHz link. We detail the observations in Sec. II and identify the root causes of significant performance disparity between best link and randomly deployed links within the same environment.

(2) An environment scoping and performance prediction framework to identify best spot of 60 GHz link deployment. The framework leverages sparsity of 60 GHz channels and spatial correlation between *spot* using a novel *environment path skeleton* model to predict the performance of unobserved but correlated spot. We present the design in Sec. III and perform preliminary experiments (Sec. IV) to validate the idea.

II. DEPLOYMENT CHALLENGES OF 60 GHZ LINKS

A LOS 60 GHz link can be extremely susceptible to human blockage if there is no secondary path for the link arrangement. Presence of reflective concrete walls, metallic cabinet *etc.* can provide significant opportunities to bounce the signals off from a secondary path in presence of large obstacles like human

body in LOS that penalizes the link by $20 \sim 30$ dB [4], [5]. We perform a measurement study to understand the impact of human blockage on arbitrarily deployed 60 GHz indoor links, and the importance of picking the right deployment spot. Our measurement uses the WiMi software radio with its default configuration (10 dBm output power, 60 GHz carrier frequency, *etc.*) [5].

A. Performance disparity between links during blockage

Despite its potential, the effectiveness of phased-array beam-steering depends on the environment [5]. Beam-steering heavily relies on the availability of secondary paths to bounce the signals in Non-Line-Of-Sight (NLOS) trajectory when the LOS is blocked.

Fig. 2 shows performance disparity during blockage across 30 different links arbitrary deployed in an indoor office environment. We deploy each link randomly in LOS with 5 m. distance between Tx and Rx. For each link, we emulate random blockage scenarios and collect performance traces of phase-array beams during blockage. Fig. 2(a) shows the fraction of complete link blackouts during blockage duration (*i.e.* no beam can sustain the connection) and we plot the CDF across the 30 links. For nodes having 32 beams, more than 50% of the links experience complete link outage at least 70% of time during human blockage. On the other hand, the difference between the fraction of time a complete link outage occurred is significant when comparing a randomly vs. best deployed link[1]. For nodes having 4 beams, this difference is only 8% but grows to 56% when the number of phased-array beams is 32. This shows that a carefully deployed link will be able to sustain connection during human blockage more effectively than a randomly deployed one. Further, deployment disparity becomes more severe when number of phased-array beams increase, which necessitate an environment-aware deployment.

Fig. 2(b) shows average number of fraction of available beams during blockage across the 30 different links. We found that as number of phased-array beams increase, more beams are available that can sustain connection (consistent with result in Fig. 2(a)). But Fig. 2(c) shows again the disparity between a best link vs. a randomly deployed link. For nodes having 4 beams, the difference of average achievable throughput is only 483 Mbps, while this difference grows to 1.7 Gbps when the number of available beam is 32! This further warrants the need of a careful 60 GHz link deployment that can not only sustain the connection more effectively during blockage.

B. Root cause

To identify the root cause of the performance disparity, we use our software radio platform to test the spatial properties of the 60 GHz links. We use a mechanical rotator to test the receiver's angular RSS distribution (*a.k.a.* AOA) while the transmitter is using an omni-directional antenna. The angular RSS distribution represents the signal arriving pattern in spatial domain. Fig. 3 showcases example tests in two locations. The

---

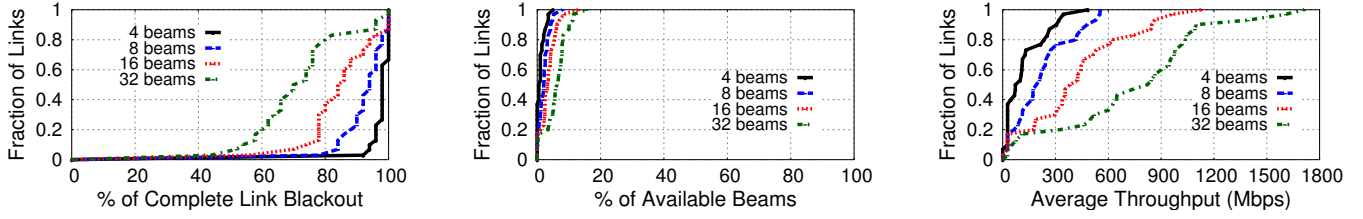[1]The link that showed best result out of all 30 links, although it may not be an oracle best link.

Fig. 2. (*a*) Fraction of complete link blackout. (*b*) Fraction of available beams. (*c*) Average throughput of best available beam when link is sustained. CDF are plotted across 30 different links during blockage.
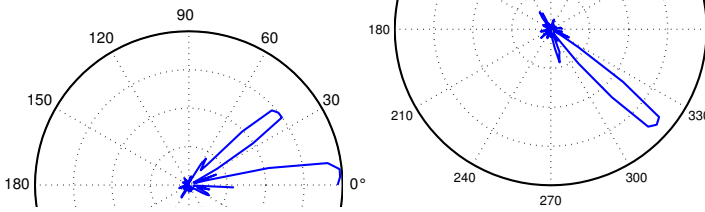

Fig. 3. Sparsity of AOA.

receiver's angular RSS is extremely sparsely distributed and signal is clustered on few narrow directions spanning a few degrees. This sparsity is due to the availability of very small number of strong reflecting objects in indoor environment. Unless the link is properly deployed to cover multiple of such clusters, lack of secondary clusters during LOS cluster blockage will cause a complete link black-out.

Although the sparse clustering of angular RSS manifests into severe disparity between the link's performance during blockage, we found it can be exploited to scope an environment for the best link placement exploiting measurement from just a single spot. (1) *Environment characterization.* Owing to the extreme sparse nature of the environment, it should be possible to characterize the full environment using few discrete paths, which we call *environment path skeleton*. (2) *Predicting performance.* It should be possible to predict the performance of unobserved spot, by modeling the way it shares the *environment path skeleton* with measured spot.

III. BEAMSCOPE DESIGN

BeamScope exploits the *sparsity* property of 60 GHz link to establish a spot performance prediction framework. The framework *determines the received signal strength (RSS) of unobserved spots' performance in an environment while observing channel information only from a single measurement spot.* *BeamScope*'s key principle lies in extracting the sparse environmental information from the measurement spot. The sparse parameters can then drive the prediction of unobserved spots. The environmental information is characterized in a novel *environment path skeleton* (EPS) model. Furthermore, modeling the way an unobserved spot shares the EPS with the measured spot, *BeamScope* can predict the performance of the unobserved spot.

BeamScope's design can be separated into two different stages: first, when user deploys the link in certain physical positions, *BeamScope* scans the environment by electronically steering pairwise Tx-Rx beams and extracts modeling parameters to construct the EPS. Next, *BeamScope* applies a spatial

transfer function over the EPS to infer how the environment should look like from any other spots within the environment.

A. Environment Path Skeleton (EPS)

BeamScope characterizes the complete environment using few discrete paths from a single measurement point. This characterization is feasible because the 60 GHz signals interacting with the environment is very sparse [6]. Formally, we define an EPS as: *the set of propagation/reflection parameters that can be used to characterize the environment from a spot, and to approximate the continuous spatial channel.*

B. Difficulty in scanning environment from single viewpoint

BeamScope's environment scanning algorithm uses reflections from the environment received via pairwise rotation of the Tx-Rx beams using static devices. However, it is technically challenging to achieve resolution accuracy beyond a meter [7]–[9] even when using high frequency like 60 GHz. The fundamental bottleneck is rooted into the limited antenna size (aperture) from a single viewpoint. Existing imaging systems like [8] use an array of virtual antennas formed from the mobility of users to improve accuracy of resolution, which again turns into laborious war-driving. In addition, it is not sufficient to estimate the distance between the environment objects but also the material characteristics as the interaction of 60 GHz signals from link depends on the diffusive property of the secondary paths which current system can not achieve.

C. Core idea: environment as a recursive diffuse mirror!

The main principle behind our environment characterization from single view-point is to extend the aperture of that view-point. *BeamScope* extends the view-point by treating environment as a *recursive diffusive mirror*.

We illustrate this idea following an example in Fig. 4, which represents a simple environment with two reflecting objects, p_i and p_j. Here, while characterizing the object p_i, we extend the aperture of the receiver Rx by considering object p_j as the diffusive mirror. The receiver Rx's aperture is now extended to fully characterize the object p_i in the environment which includes estimating the distance and the diffusion coefficient. Similarly, while characterizing p_j, p_i is considered as the diffusive mirror.

D. Prediction Framework: Model & Algorithm

The *BeamScope* prediction framework builds on the core idea to first characterize environment and leverage it to predict performance of unobserved spot within the environment.
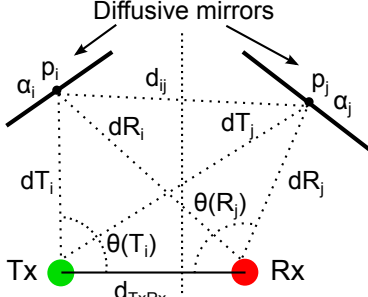
Fig. 4. Environment as a recursive diffusive mirror.

1) Constructing the Environment Path Skeleton: When the 60 GHz devices are deployed at certain positions, *BeamScope* invokes a full beam-scanning procedure (such as in 802.11ad) once to capture the *Channel Impulse Response* (CIR) between each pair of Tx/Rx beams. *BeamScope* then uses matrix $\mathbf{M}$ of $K \times K$ entries to store the CIR of the K received beams from each of the K transmit beam.

When the narrow beam of 60 GHz transmitter incident on an object in the environment, it creates the first signal bounce. This direct bounce is followed by a complex pattern of inter-reflections whose dynamics are governed by the environment geometry and the diffusion property of the material in the environment. At any time instant the receiver observes a projection of the complete set of paths from the environment and this comprises only the paths that are directed towards the receiver and within it receive beam space.

Now, lets consider environment $\mathbb{E}$ comprise of K planar objects $\{p_1, p_2, \ldots, p_K\}$. Let Euclidean distance vector $\mathbf{dT} = \{dT_1, dT_2, \ldots, dT_K\}$ and $\mathbf{dR} = \{dR_1, dR_2, \ldots, dR_K\}$ denote distance between the planar objects and transmitter and receiver respectively. In addition, let the diffusion coefficient of each planar point be denoted by α_i, which refers to amount of signal reflected from the point towards direction i. We assume that signals in rest of the directions is uniformly distributed with signal energy being fraction $(1-\alpha_i)$ of the original signal energy. Also, consider $\mathbf{D} = [d_{ij}]$ to be the pairwise distance between the planar objects. The EPS is the vector that stores $[\mathbf{dT}, \mathbf{dR}, \alpha]$ comprised of distance of planar object from the transmitter, receiver and the diffusivity.

BeamScope constructs the EPS using the CIR matrix M. Simply put, each CIR entry m_{ij} in $\mathbf{M}$ contains information about the complete path traversed by the 60 GHz signal which was emitted from a narrow beam i at Tx and captured using a narrow beam j at Rx. Fig. 4 shows an example of the path level model. The captured CIR provides with RSS and phase information of signal that interacted and modulated by the environment. To put it concretely, the RSS/phase of the 60 GHz signal transmitted from beam direction T_i and received by beam direction R_j contains information about the distance of Tx from the planar object p_i, the inter-distance between the object p_i and p_j, distance of Rx from p_j and the diffusion coefficient α_i and α_j.

Therefore, the amplitude $A(\cdot)$ and phase $\Phi(\cdot)$ of CIR m_{ij} is modeled as,

$$A(m_{ij}) = \frac{\alpha_i \cdot \alpha_j}{dT_i^2 \cdot d_{ij}^2 \cdot dR_j^2}$$
$$\left(n_{ij} + \frac{\Phi(m_{ij})}{2\pi}\right) \cdot \lambda = dT_i + d_{ij} + dR_j \qquad (1)$$

Where n_{ij} is the unknown number of full 2π phase rotations that occurred when the rays traveled from Tx to Rx covering distances dT_i, d_{ij} and dR_j. In addition, the cosine rule from Fig. 4 gives,

$$dR_i^2 = dT_i^2 + d_{TxRx}^2 - 2 \cdot dT_i \cdot d_{TxRx} \cdot cos(\theta(T_i))$$
$$dT_j^2 = dR_j^2 + d_{TxRx}^2 - 2 \cdot dR_j \cdot d_{TxRx} \cdot cos(\theta(R_j)) \qquad (2)$$

We extract the vector $[\mathbf{dT}, \mathbf{dR}, \alpha]$ by jointly solving equations (1) and (2) for all $i = 1, 2, \ldots, K$ and $j = 1, 2, \ldots, K$. By default, we assume that there are up to K planar objects present in the environment (where K is the number of available Tx/Rx beams) and thus the total number of unknown variables to solve for and the number of equations is $2 \cdot K \cdot (K+1)$ and $2K^2$ respectively. The exact solution for the EPS vector is not easy to extract as the above system of equations is underdetermined. We approximate the solution by leveraging *Levenberg-Marquardt Algorithm (LMA)* [10] , which are widely applied in solving non-linear inverse problems. Since in a typical indoor environment the number of strong 60 GHz reflectors are very limited [5], [6], [11], the above solution space is feasible even for a limited number of available beams.

2) Predicting the Performance of Unobserved Spot: The EPS captures the snapshot of the environment and how a 60 GHz link interacts with it. Therefore, to predict performance in an unobserved spot is to predict how the environment snapshot is supposed to look like from that spot. Specifically, we assume that location of the spot where we want to predict the performance is known to *BeamScope*. To simplify the exposition, we assume that we only want to predict unobserved Rx spot, *i.e.*, Tx is now fixed. Further, the coordinate of the unobserved spot is assumed to be known, denoted as (x_s, y_s) *w.r.t.* the reference coordinate (the position of the Tx). Therefore, predicted EPS from the unobserved spot is given by, $[\mathbf{dT}, \mathbf{Tr}_R(\mathbf{dR}), \alpha]$, where $\mathbf{Tr}_R(\mathbf{dR})$ denotes the new distance metric between the planar reflectors and the new receiver position (x_s, y_s). Given that we known the distance metric from the reflectors to the reference Rx, we can use standard geometrical manipulations to get the new distance metric. Finally, this new distance metric is converted to the angular RSS (AOA) pattern using Eq. (1).

IV. EVALUATION

We evaluate the feasibility of *BeamScope* using a combination of channel traces and simulation. The channel traces are collected on a 60 GHz software radio platform [5] which allows programmable waveform generation and received-signal processing on a PC host. We use a motion control system and directional antenna (3°) to capture the pairwise channel response of a Tx-Rx of a 60 GHz link, in a similar way as [6]. The channel response are used to construct environment
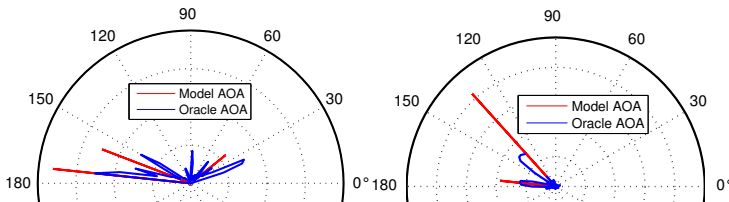
Fig. 5. Examples of predicting the AOA from Environment Path Skeleton.

path skeleton and corresponding predict the performance of an arbitrary unobserved spot.

We evaluate the feasibility of *BeamScope* in predicting the performance of unobserved from 2 aspects. (1) How accurately *BeamScope* can predict the AOA? (2) What is the accuracy in predicting the performance of best beam?

A. Predicting AOA

We test the accuracy of *BeamScope* in predicting the angular RSS distribution of unobserved spot from measurement results obtained from a reference link deployment. We deploy the reference link in an indoor office environment and measure the CIR matrix by steering across multiple beam patterns. This measurement is used to construct the environment path skeleton as per Sec. III-D.1. Further, we move the receiver randomly in 8 different spots, noted the physical distance from the original receiver spot and collect there angular RSS that serve as oracle measurement. The modeled environment path skeleton is used to predict the performance in those 8 random spots and compared the result *w.r.t.* the oracle measurement. Fig. 5 showcases two examples of predicting the AOA. For the first case, there were two very close-by reflectors along with the clutters in the office space, while the second case is without the clutters and similar to the illustrative Fig. 4.

B. Accuracy in predicting performance of best beam

We compare the prediction accuracy of finding the best beam index in the unobserved spots and Fig. 6 shows the accuracy with varying number of available phased-array beams at the receiver side. The accuracy drops as the number of available beams increase. The main reason behind that the AOA in unobserved spots is approximated by modeling sparse set of paths and this approximation error manifests into larger error in identifying best beam among adjacent beams.
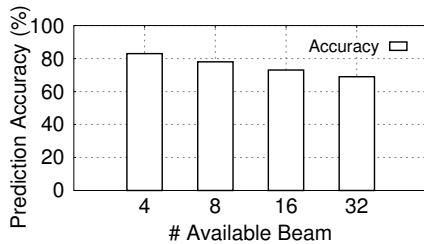

Fig. 6. *BeamScope*'s best beam prediction accuracy.

C. Spatial prediction accuracy

To evaluate the feasibility of *BeamScope* in large-scale, we evaluate the prediction algorithm through simulation. We follow the approach in [12] and simulate the signal propagation of a 60 GHz link in an indoor room (dimension: $10m \times 10m$),
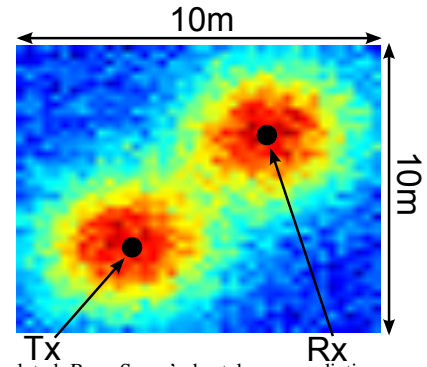

Fig. 7. Simulated *BeamScope*'s best beam prediction accuracy in spatial region. Reference Tx and Rx placement is shown. Dark color represents higher accuracy.

with 3 concrete reflectors deployed randomly. The reflective coefficients are chosen from [13]. We fixed the reference spot of the link and compared the modeled and measured best beam's prediction accuracy. Fig. 7 shows a heatmap of the prediction accuracy of finding the best beam in unobserved *spots* using measurement only from the reference link spot.

This simulation result demonstrates that the accuracy becomes higher as we move closer to the reference link. It also suggests the need for collecting measurement from multiple reference *spots* in order to cover the whole indoor area, which we have planned in our future work.

V. DISCUSSIONS AND FUTURE WORK

Guided measurement for full room coverage. Our current design does not allow to perceive a true depth of the scene geometry like a 3D camera based system. Irrespective of that, the AOA prediction still shows promising result because the interaction of 60 GHz signal with the environment depends not only on the distance of the objects but also the diffusive characteristic of the material. As the spatial AOA of any arbitrary deployment point in the space is jointly affected by the distance of the reflector and the diffusivity of it, we can still predict the AOA by solving the system of nonlinear equations. However, due to the distorted depth-perception, the physical space within which the performance prediction works becomes limited and may potentially create *prediction coverage holes w.r.t.* the oracle room geometry. In future, we plan to solve this problem by potentially sampling a few other points in the pre-deployment stage. We plan to design an *Expectation Maximization* algorithm that quickly sieves the *prediction coverage hole* in the environment and guide the user to sample the environment fully.

True depth-perception exploiting Gbps channel impulse response. Our current hardware does not support Gbps bandwidth and a sub-nanosecond timing resolution of received signal can not be achieved. Current 802.11ad standard supports 2.16 GHz bandwidth and correspondingly a fine-grained timing information from the channel impulse response can potentially be plugged in the system of nonlinear equations in order to better estimate distance/diffusion coefficients and resolve any depth aliasing. This can potentially solve the *prediction coverage hole* problem described above without the

need for multiple sampling points in the pre-deployment stage. In future, we plan to make software-radio platform's capability comparable to an 802.11ad system and enable more accurate depth-estimation.

3D environment scoping. Current *BeamScope* algorithm is applicable to scope single planar objects in azimuthal plane. We believe that it is sufficient for first order approximation of best possible *spot* and the experimental result shows promising accuracy. However, a 3D scoping of the environment in both azimuthal and elevation plane should provide more accurate result. We plan to explore 3D environment scoping and prediction in our future work.

VI. RELATED WORK

Commercial ranging devices, *e.g.*, RangeFinder [14], use phase shifts information of two or more low modulating frequencies over laser pulse beams to accurately measure the distance of remote objects with mm. level accuracy. Time-of-Flight camera which can provide richer information like arrival rates of light photons reflected from objects, can be used to estimate short distances at sub-nm. accuracy. Kirmani *et al.* [15] and Heide *et al.* [16] used impulse response from multi-order reflections of light photons to estimate the 3D geometry of objects inside a room. In addition, a conventional 3D camera uses dual perspectives of the same pixel to generate 3D view of the environment. Unlike *BeamScope*, none of the method described above can estimate the depth as well as material characteristics (*e.g.* diffusive property) of different objects in the environment, which is essential for predicting signal AoA for an unobserved location. Further, the diffusive property of material at 60 GHz frequency spectrum is significantly different from light spectrum. Thus, camera-based imaging result can not be directly applied in our problem setup.

Recent work explored *acoustic room impulse response* to estimate the room dimensions [17]–[19] and object shape [20] in the environment. However, such solutions are not directly applicable to 60 GHz networks, which require not only the understanding of scene geometry but also the reflective/diffusive property of the material at 60 GHz.

An alternative way of mapping the environment is mmWave imaging. Conceptually, one can move the mmWave radio around and generate an image similarly to synthetic aperture radar [21]. However, this requires laborious war-driving, and requires the radio location to be known at millimeter-precision. Such setup is challenging and unnecessary — given that the environment is sparse, it is sufficient to sparsely sample the environment and map the major reflectors, as done in *BeamScope.*

VII. CONCLUSION

We have designed and evaluated the feasibility of *BeamScope*, a system that scopes the environment to scour best possible location to deploy a 60 GHz link in indoor environment. *BeamScope* characterizes the environment by capturing sparse path metric in a measurement-based and model-driven framework. Further, it models the way the metric is shared between unobserved and reference locations and exploits this information to predict the performance in unobserved locations. While the preliminary results evaluated in a software-radio platform shows potential, we believe *BeamScope*'s accuracy can be increased via a higher-dimension model, which we plan to investigate in our future work.

REFERENCES

[1] IEEE Standards Association, "IEEE Standards 802.11ad-2012: Enhancements for Very High Throughput in the 60 GHz Band," 2012.

[2] ——, "IEEE Standards 802.15.3c-2009: Millimeter-wave-based Alternate Physical Layer Extension," 2009.

[3] "Wilocity 802.11ad Multi-Gigabit Wireless Chipset," http://wilocity.com, 2013.

[4] S. Collonge, G. Zaharia, and G. Zein, "Influence of the Human Activity on Wide-Band Characteristics of the 60 GHz Indoor Radio Channel," *IEEE Trans. on Wireless Comm.*, vol. 3, no. 6, 2004.

[5] S. Sur, V. Venkateswaran, X. Zhang, and P. Ramanathan, "60 GHz Indoor Networking through Flexible Beams: A Link-Level Profiling," 2015, proc. of ACM SIGMETRICS.

[6] S. Sur, X. Zhang, P. Ramanathan, and R. Chandra, "BeamSpy: Enabling Robust 60 GHz Links Under Blockage," in *Proc. of USENIX NSDI*, 2016.

[7] Y. K. Chan and V. C. Koo, "An Introduction to Synthetic Aperture Radar (SAR)," vol. 2, no. 1, 2008.

[8] Y. Zhu, Y. Zhu, Z. Zhang, B. Y. Zhao, and H. Zheng, "60 GHz Mobile Imaging Radar," in *HotMobile*, 2015.

[9] D. Huang, R. Nandakumar, and S. Gollakota, "Feasibility and Limits of Wi-Fi Imaging," in *SenSys*, 2014.

[10] C.-T. Kim, J.-J. Lee, and H. Kim, "Variable Projection Method and Levenberg-Marquardt Algorithm for Neural Network Training," in *IEEE Industrial Electronics (IECON)*, 2006.

[11] H. Xu, V. Kukshya, and T. Rappaport, "Spatial and Temporal Characteristics of 60-GHz Indoor Channels," *IEEE Journal on Selected Areas in Communications*, vol. 20, no. 3, 2002.

[12] H. Deng and A. Sayeed, "Mm-Wave MIMO Channel Modeling and User Localization Using Sparse Beamspace Signatures," in *IEEE International Workshop on Signal Processing Advances in Wireless Communications (SPAWC)*, 2014.

[13] B. Langen, G. Lober, and W. Herzig, "Reflection and Transmission Behaviour of Building Materials at 60 GHz," in *IEEE PIMRC*, 1994.

[14] Bosch, "Bosch DLE 40 Professional," 2015. [Online]. Available: http://www.bosch-pt.com.ph/ph/en/laser-measure-dle-40-131500.html

[15] A. Kirmani, T. Hutchison, J. Davis, and R. Raskar, "Looking Around the Corner using Transient Imaging," in *IEEE International Conference on Computer Vision (ICCV)*, 2009.

[16] F. Heide, L. Xiao, W. Heidrich, and M. B. Hullin, "Diffuse Mirrors: 3D Reconstruction from Diffuse Indirect Illumination using Inexpensive Time-of-Flight Sensors," in *IEEE Conference on Computer Vision and Pattern Recognition (CVPR)*, 2014.

[17] E. A. Lehmann and A. M. Johansson, "Prediction of energy decay in room impulse responses simulated with an image-source model," *The Journal of the Acoustical Society of America*, vol. 124, no. 1, 2008.

[18] D. Marković, F. Antonacci, A. Sarti, and S. Tubaro, "Estimation of Room Dimensions from a Single Impulse Response," in *IEEE Workshop on Applications of Signal Processing to Audio and Acoustics (WASPAA)*, 2013.

[19] I. Dokmanić, R. Parhizkar, A. Walther, Y. M. Lu, and M. Vetterli, "Acoustic Echoes Reveal Room Shape," in *Proceedings of the National Academy of Sciences of the United States of America*, 2013.

[20] C.-Y. Lee, L. Yan, and S.-R. Lee, "Estimation of Inclination Angle of a Planar Reflector Using Sonar Sensor," *IEEE Sensors Journal*, vol. 7, no. 7, 2007.

[21] M. Cheney and B. Borden, *Fundamentals of Radar Imaging*. Society for Industrial and Applied Mathematics, 2009.